Source process and scaling of small earthquakes

Hisao Ito[1], Kazutoshi Imanishi[1], Anna Stork[1], William L. Ellsworth[2], and Shinobu Ito[1]

Geological Survey of Japan/AIST[1]
U.S.Geological Survey[2]

4th UJNR Meeting, Nov. 6-8, 2002, Morioka, Japan

The same scaling law for large earthquakes and small earthquakes?

Breakdown?

(Kanamori and Heaton, 2000)

Although the determination of M_0 can be made accurately, the determination of E_R is still subject to large uncertainties. The values of E_R estimated for the same earthquake by different investigators often differ by more than a factor of 10 [*Singh and Ordaz*, 1994; *Mayeda and Walter*, 1996]. In particular, the values determined from

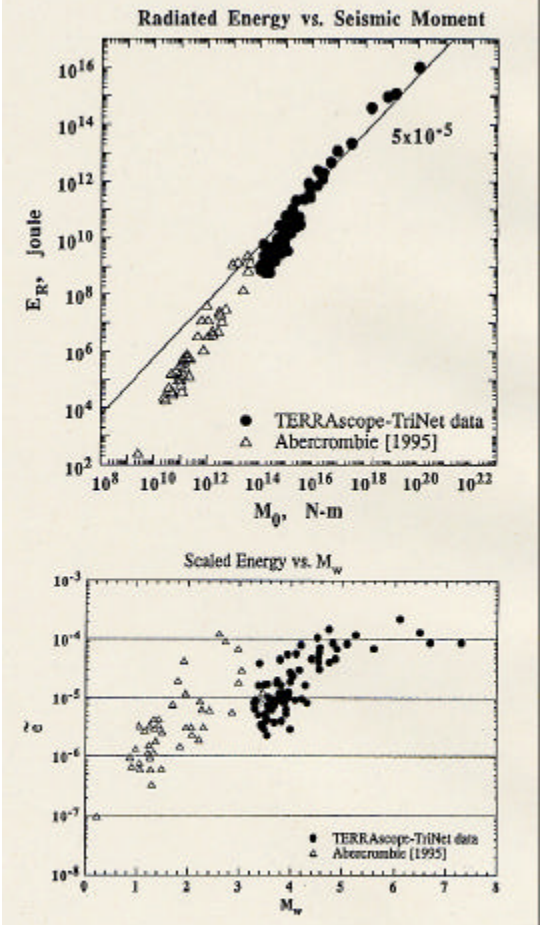

Figure 5. a). Relation between the radiated energy E_R and the seismic moment M_0. The data for large earthquakes (solid circle) are from southern California [updated from *Kanamori et al.*, 1993], and those for small earthquakes (open triangles) are taken from *Abercrombie* [1995]. b) The scaled energy, $\tilde{e}=E_R/M_0$, computed as a function of M_W. Note that the values of $\tilde{e}$ for small earthquakes are 10 to 100 times smaller than those for large earthquakes.

Breakdowns are artifacts due to missing energy problem? (Ide and Beroza, 2001)

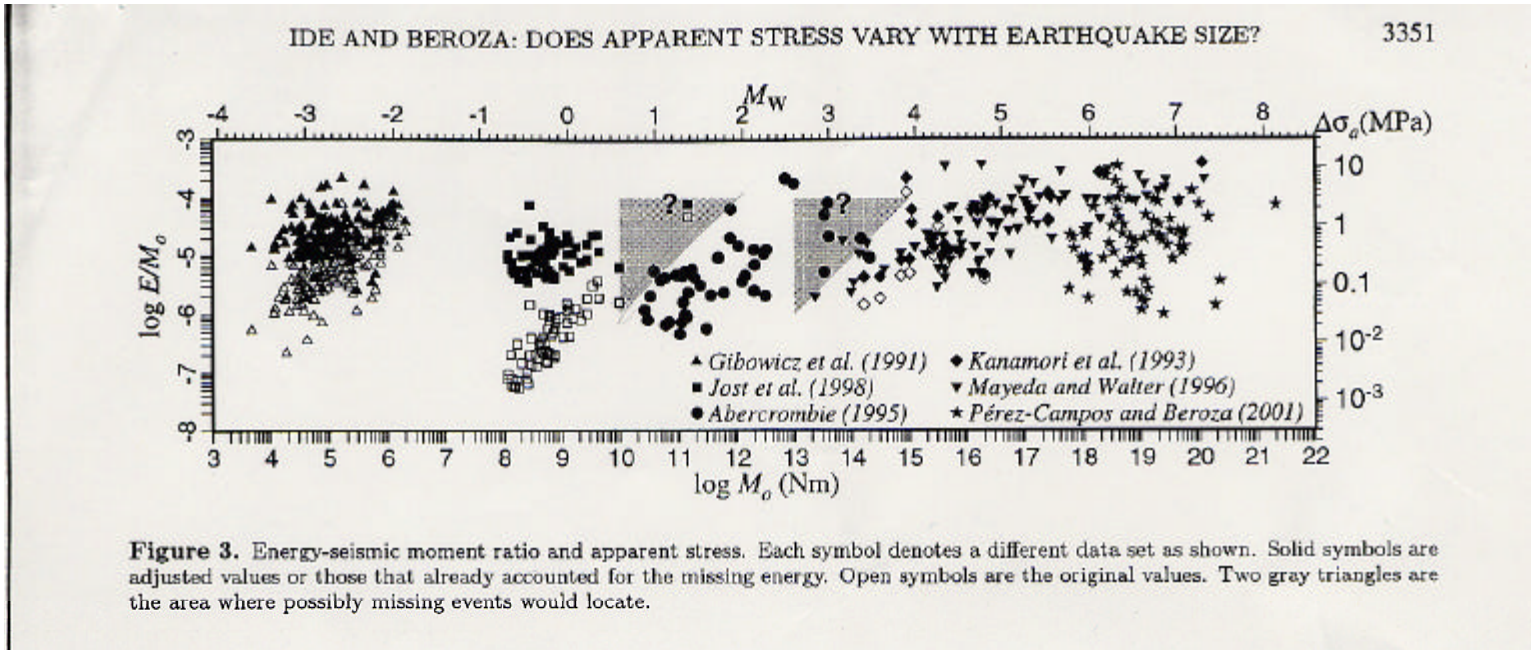

Figure 3. Energy-seismic moment ratio and apparent stress. Each symbol denotes a different data set as shown. Solid symbols are adjusted values or those that already accounted for the missing energy. Open symbols are the original values. Two gray triangles are the area where possibly missing events would locate.

Previous works

Abercrombie(1995)

Prejean and Ellsworth(2001)

Frequency domain

Q

No breakdown

Problems

The higher frequencies needed to define source characteristics of small earthquakes are most affected by attenuation along the ray path and by near-surface site effects.

Western Nagano

Shallow seismic activity

Borehole in the vicinity of the hypocenters

High frequency data sampling

Western Nagano region

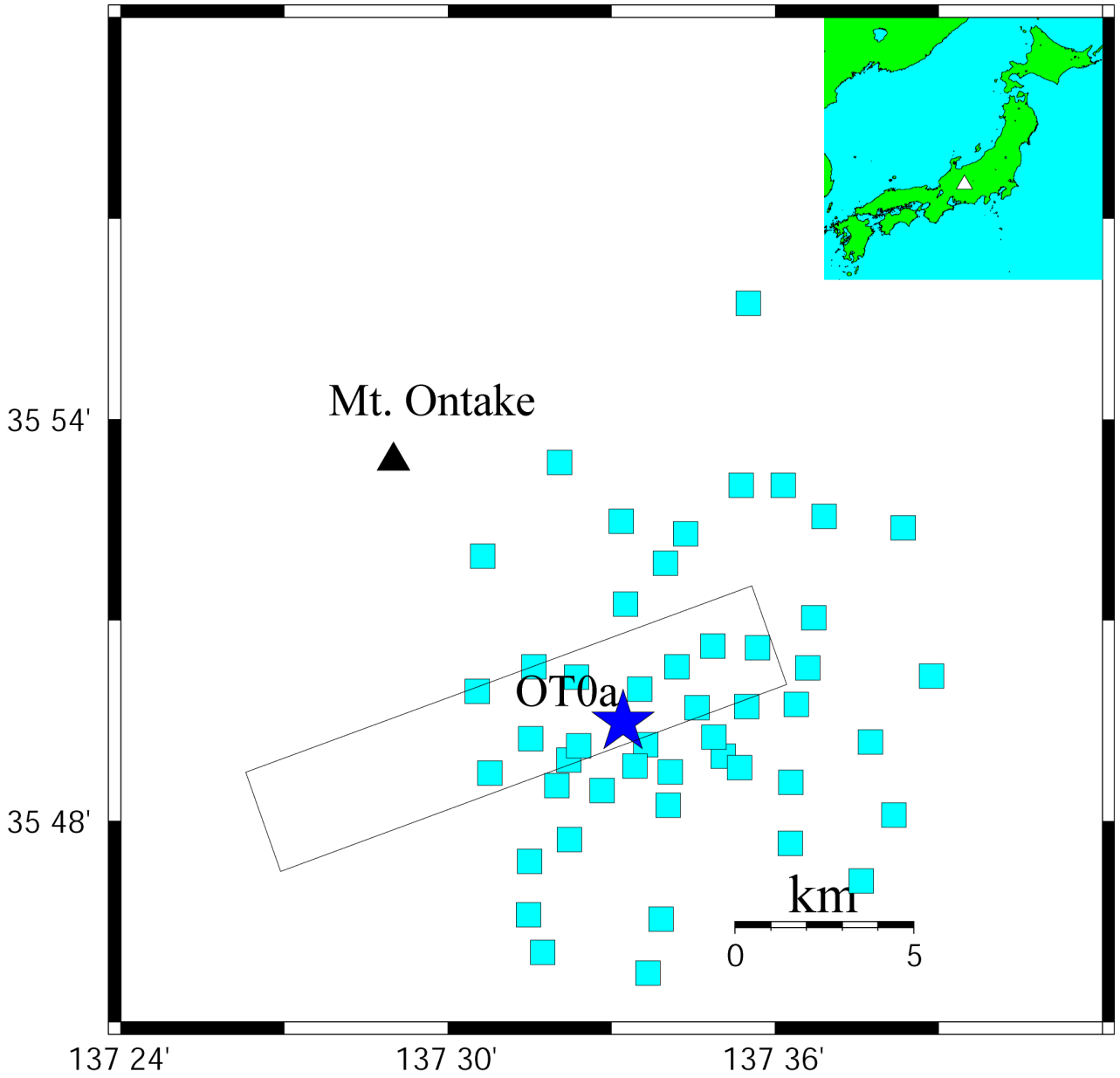

Wettern Nagano

Shallow seismicity
GSJ Borehole with 3-component seismometer (2Hz velocity)

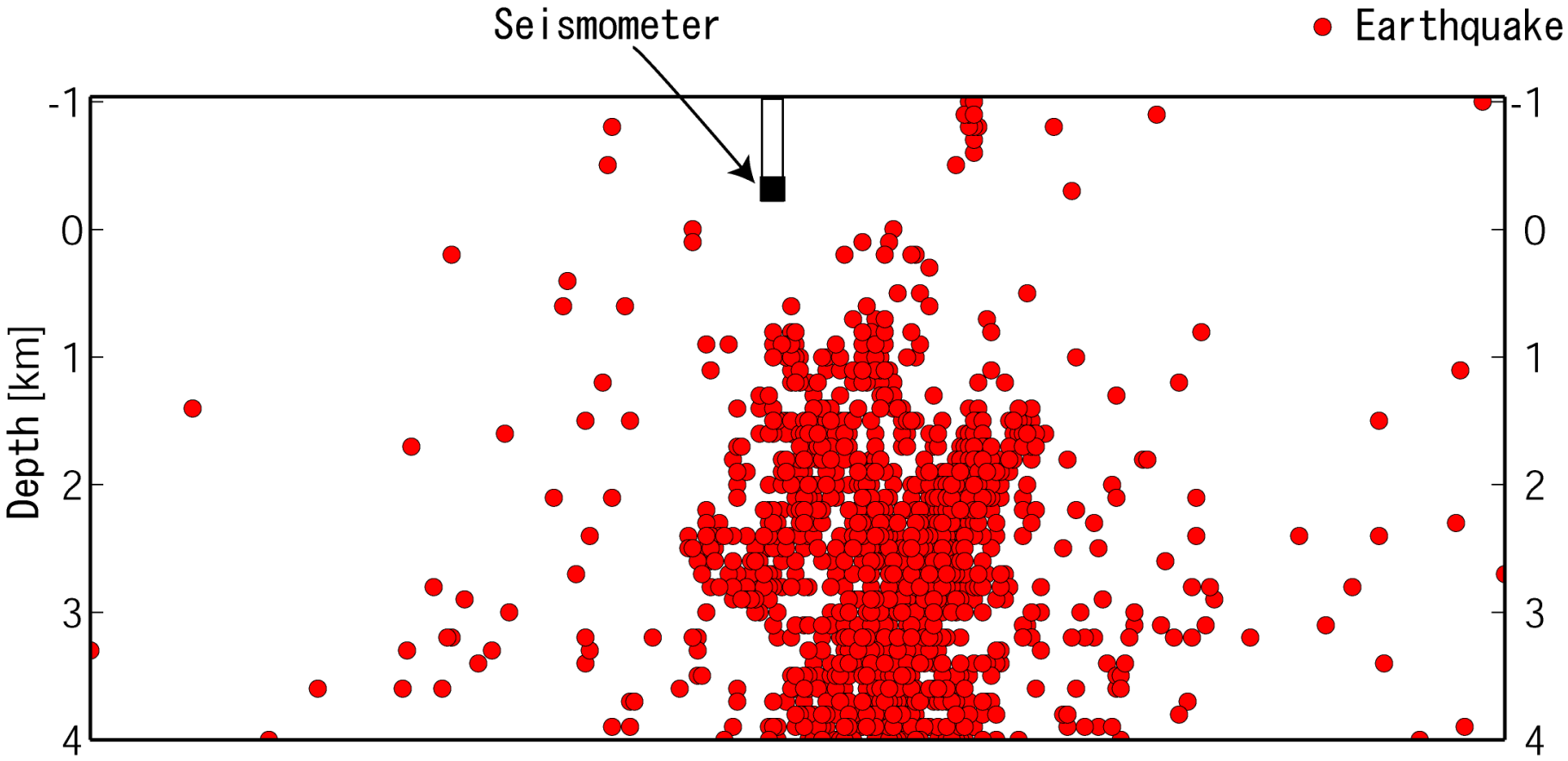

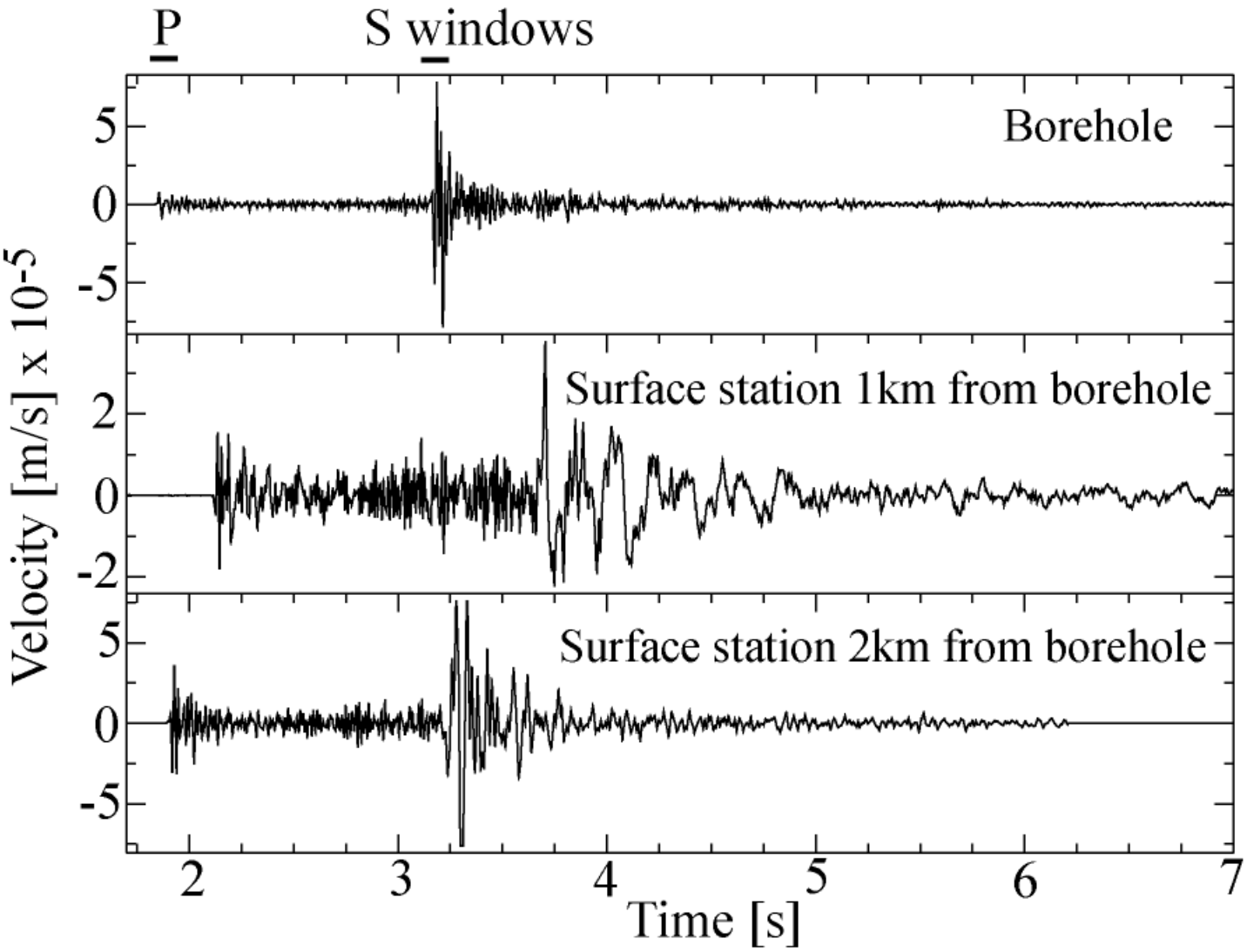
P
S windows
Borehole
Surface station 1km from borehole
Surface station 2km from borehole
Velocity [m/s] x 10-5
Time [s]
5
0
-5
2
0
-2
5
0
-5
2
3
4
5
6
7

Analysis

1. Frequency domain

Spectrum analysis

2. Time Domain

Stopping phase

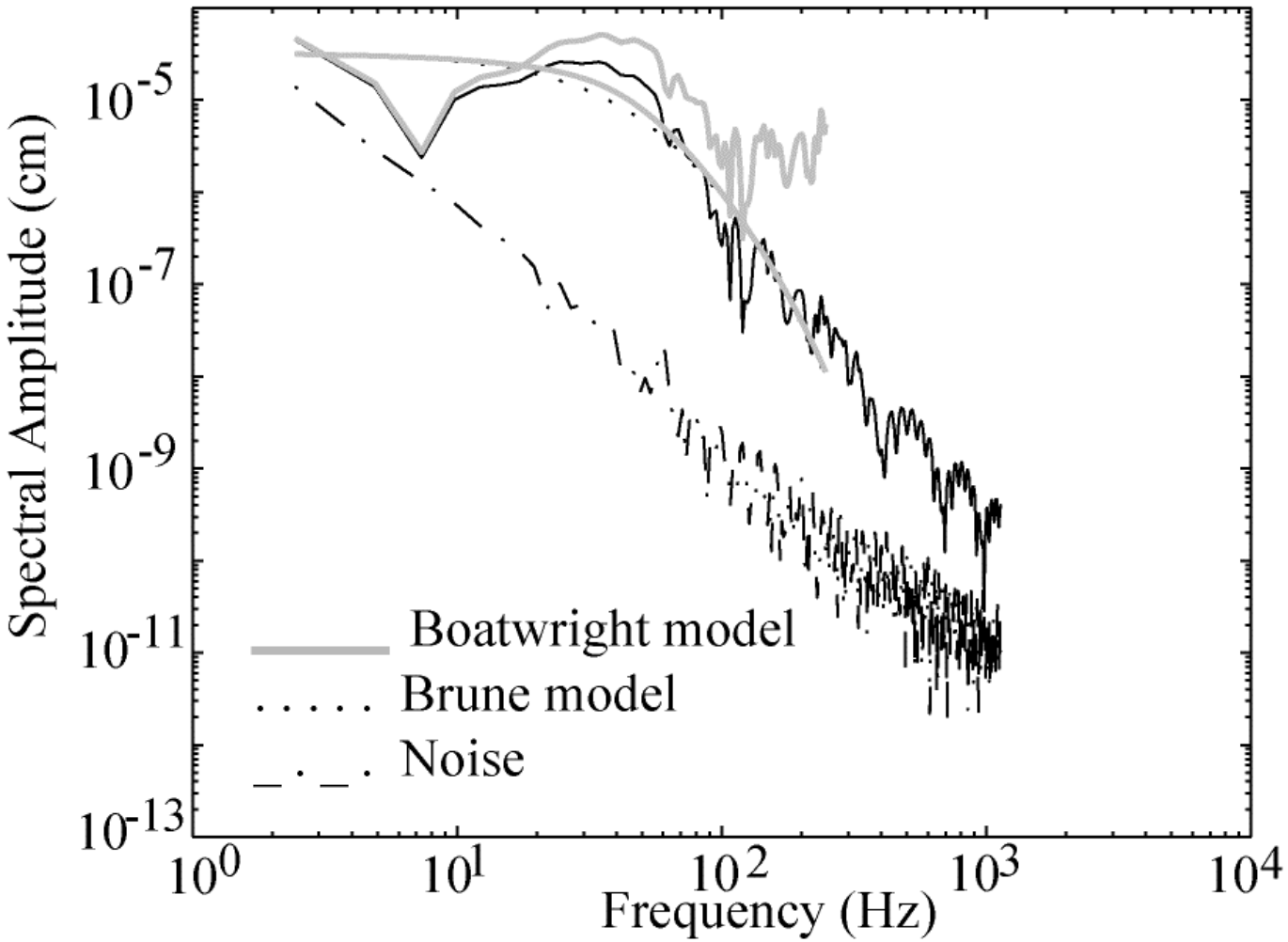
Spectral Amplitude (cm)
10-5
10-7
10-9
10-11
10-13
100
101
102
103
104
Frequency (Hz)
Boatwright model
Brune model
Noise

Constant Q?

Abercrombie(1995)

Prejean and Ellsworth(2001)

Constant Q →No Breakdown

Frequency dependent Q?

Constant Q

$$\Omega(f) = \frac{\Omega_0 \exp^{\frac{-pft}{Q}}}{\left[1+\left(f/f_c\right)^2\right]}$$

$$M_o = \frac{4prv^3 d\Omega_o}{F}$$ Brune (1970)

$$E_s = \frac{4prvd^2\langle F\rangle^2 \int \dot{u}^2 df}{F^2}$$ Boatwright and Fletcher (1984)

No change between two :
Brune (1970) and Boatwright and Fletcher (1984)

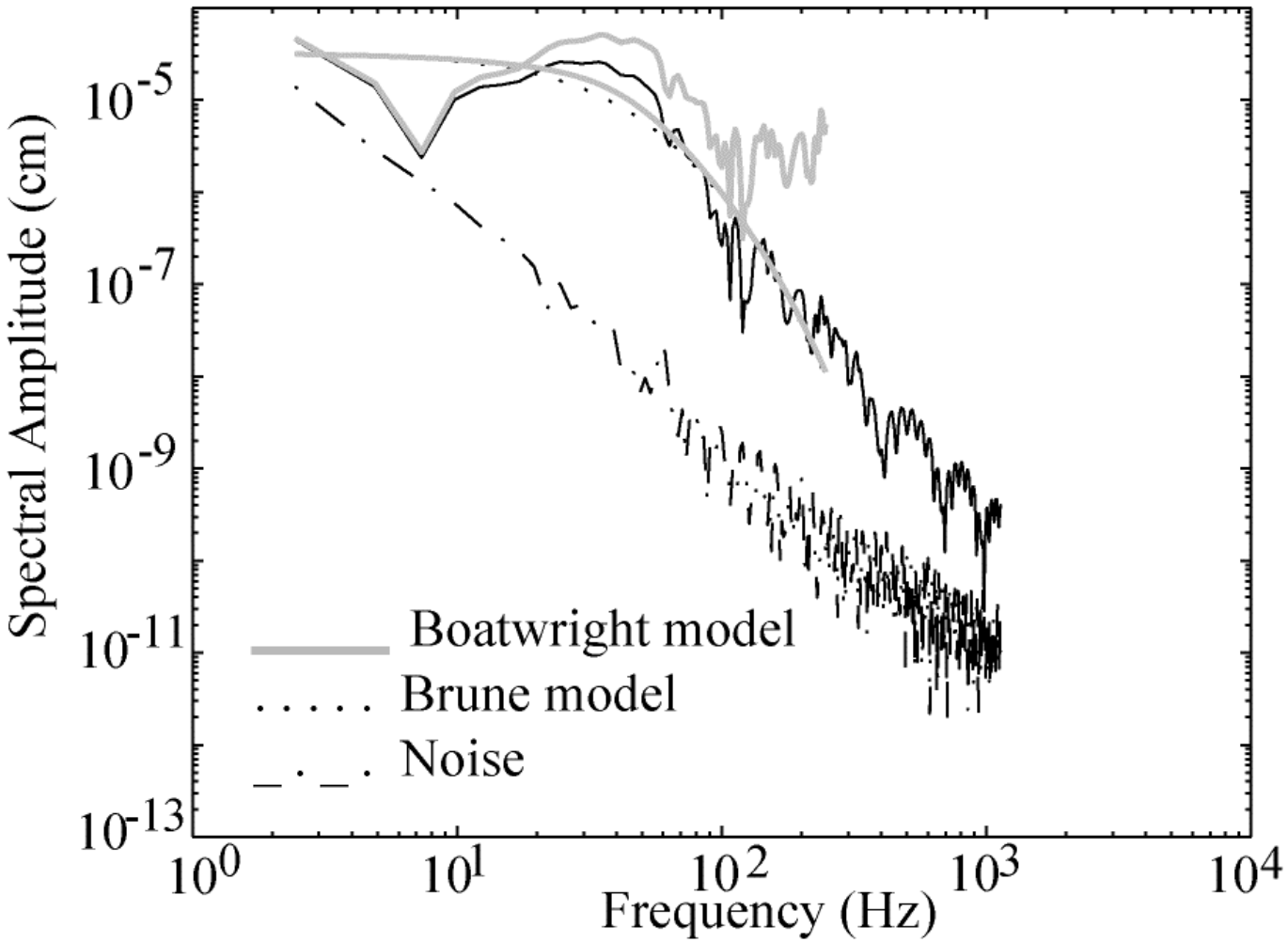
Spectral Amplitude (cm)
10-5
10-7
10-9
10-11
10-13
100
101
102
103
104
Frequency (Hz)
Boatwright model
Brune model
Noise

Q from constant Q analysis Qp=293, Qs=560

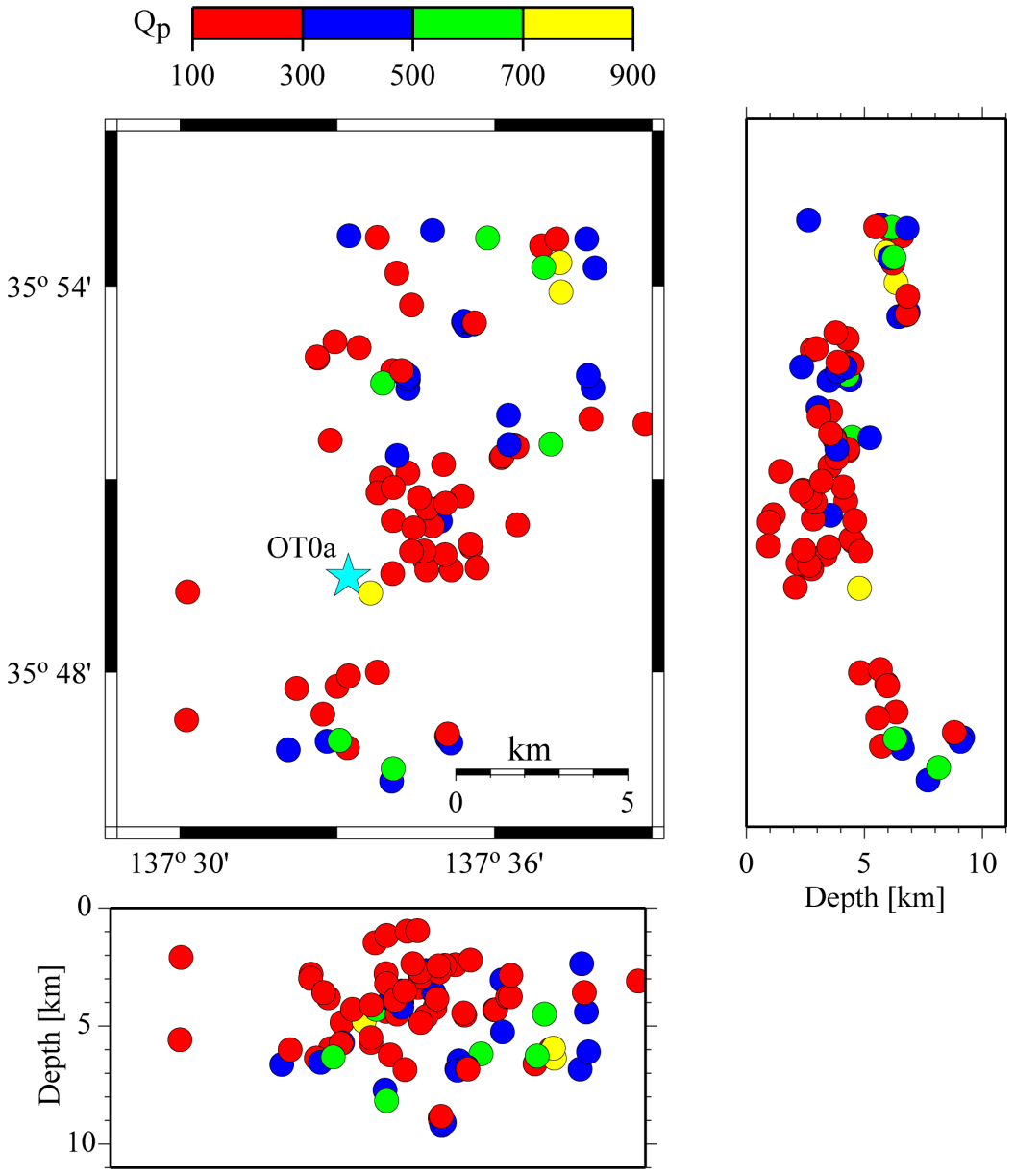

Frequency dependent Q: coda normalization method

$$\ln\left[\frac{A_p(f,d)d}{A_C(f,t_C)}\right] = \frac{pf}{Q_p(f)v_p} + c_p(f)$$

$$\ln\left[\frac{A_s(f,d)d}{A_C(f,t_C)}\right] = \frac{pf}{Q_s(f)v_s} + c_s(f)$$

$$Q_p = 73 \qquad f < 10$$
$$Q_p \approx 9.255 f^{0.9019} \qquad 10 \le f \le 60$$
$$Q_p = 372 \qquad f > 60$$

$$Q_s = 109 \qquad f < 10$$
$$Q_s \approx 12.620 f^{0.9355} \qquad 10 \le f \le 60$$
$$Q_s = 581 \qquad f > 60$$

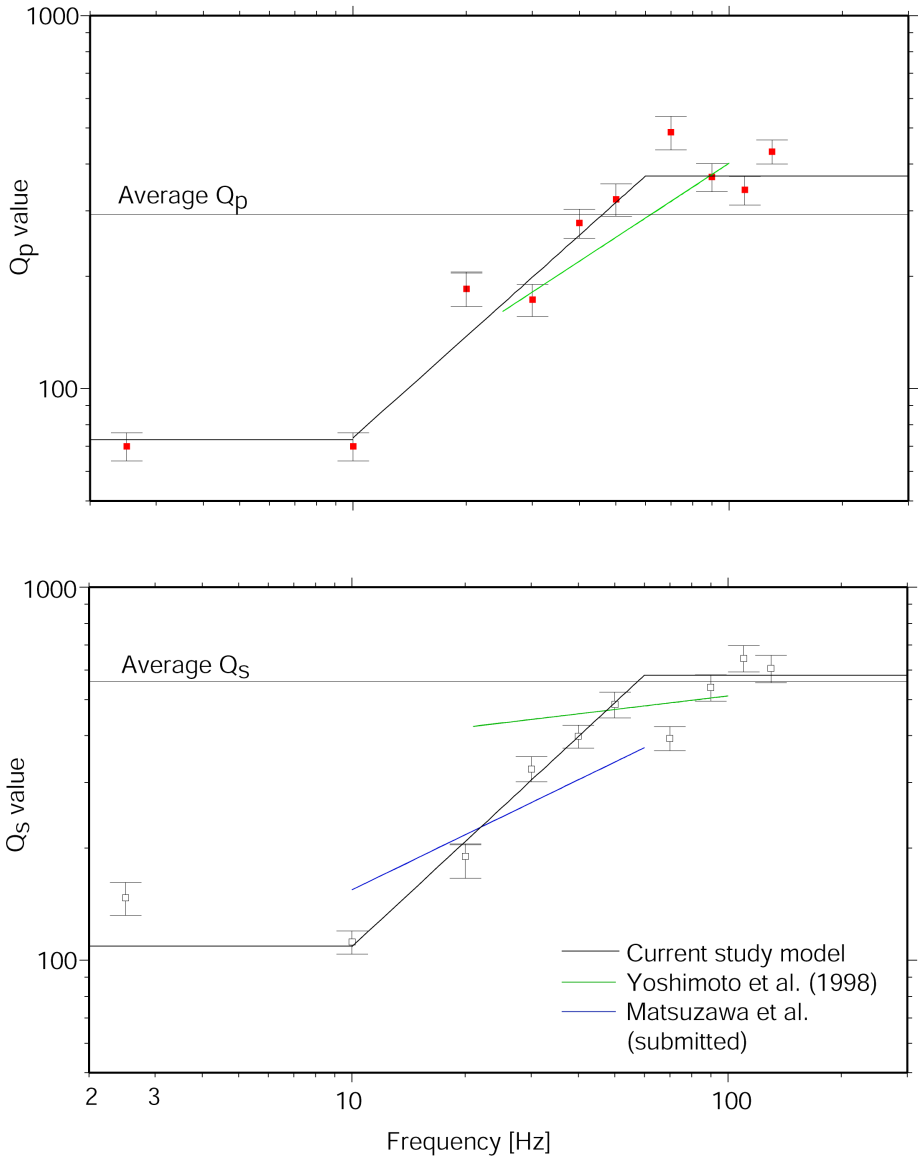
1000
100
Average Q_p
Q_p value
1000
100
Average Q_S
Q_S value
Current study model
Yoshimoto et al. (1998)
Matsuzawa et al. (submitted)
2
3
10
100
Frequency [Hz]

Results from spectral analysis

- Constant Q , Q (f)
- Recording limit

  corrected
- Window length
- Location dependence: hypocentral distance

＜7 km ＜ Mw 1.6

＜ 10 km 1.6 ＜ Mw ＜ 3.0

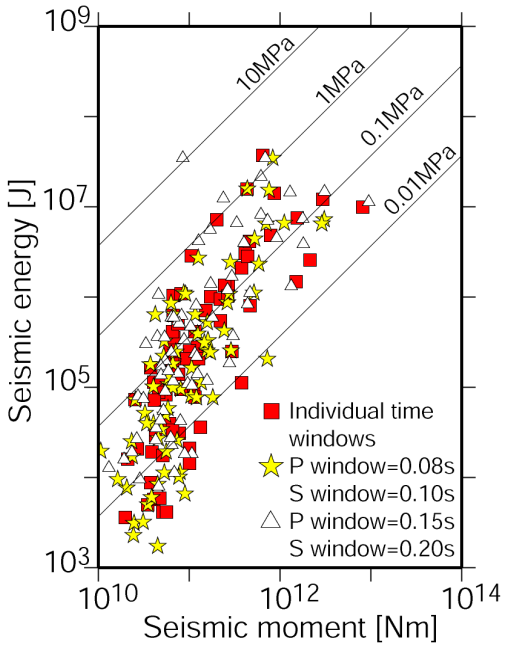
10MPa
1MPa
0.1MPa
0.01MPa
Individual time windows
P window=0.08s
S window=0.10s
P window=0.15s
S window=0.20s
Seismic energy [J]
Seismic moment [Nm]
10^9
10^7
10^5
10^3
10^10
10^12
10^14

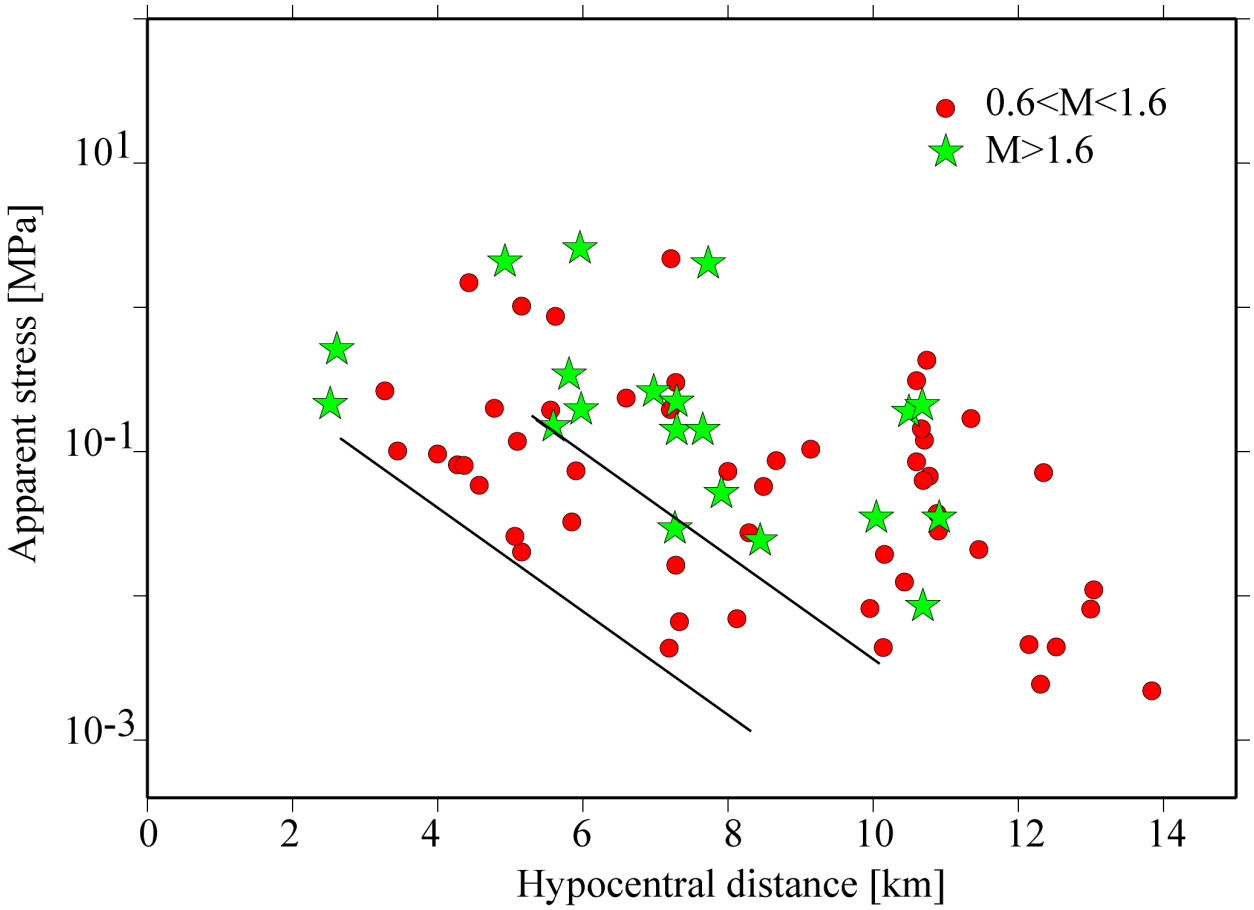
0.6<M<1.6
M>1.6
Apparent stress [MPa]
10^1
10^-1
10^-3
0
2
4
6
8
10
12
14
Hypocentral distance [km]

Locations of earthquakes

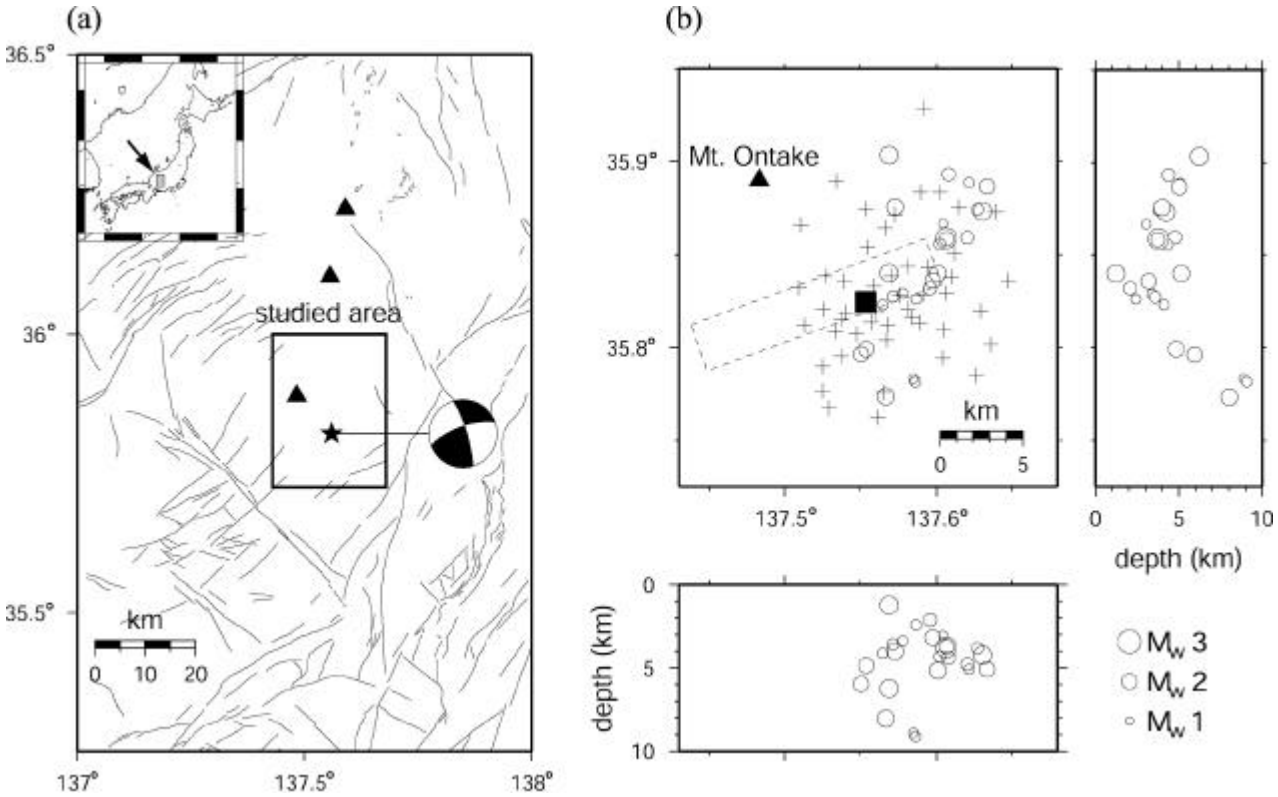

Elliptical fault model

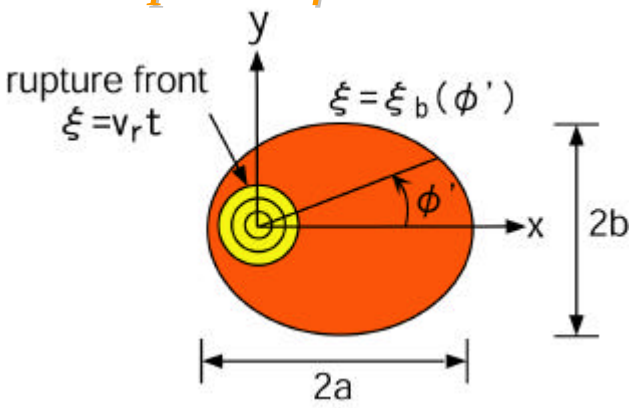

Accelerograms

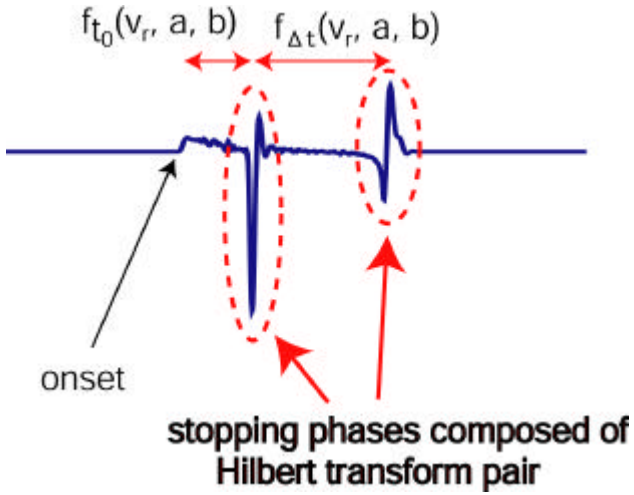

Mutual relation of Hilbert transform pair

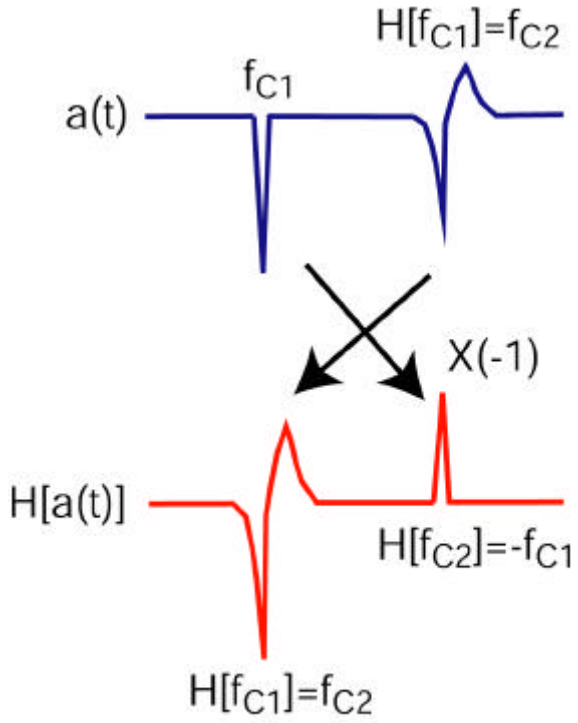

H[ ]: Hilbert transformation

Estimation of source parameters

- The inversion method used in this study is presented by Imanishi and Takeo (2002). They showed that the rise time and the difference in arrival times between the two stopping phases are dependent on the average value of the rupture velocity, the radius of the major and minor semi-axes of the ellipse , its ellipticity, the rupture direction, and the orientation of the fault plane.

- The data in the inversion consist of the difference in arrival time between the two stopping phases , the P-wave rise time and S-wave rise time for the 800 m borehole station, and the P-wave rise times (,) for other stations. Thus the total number of the data is .

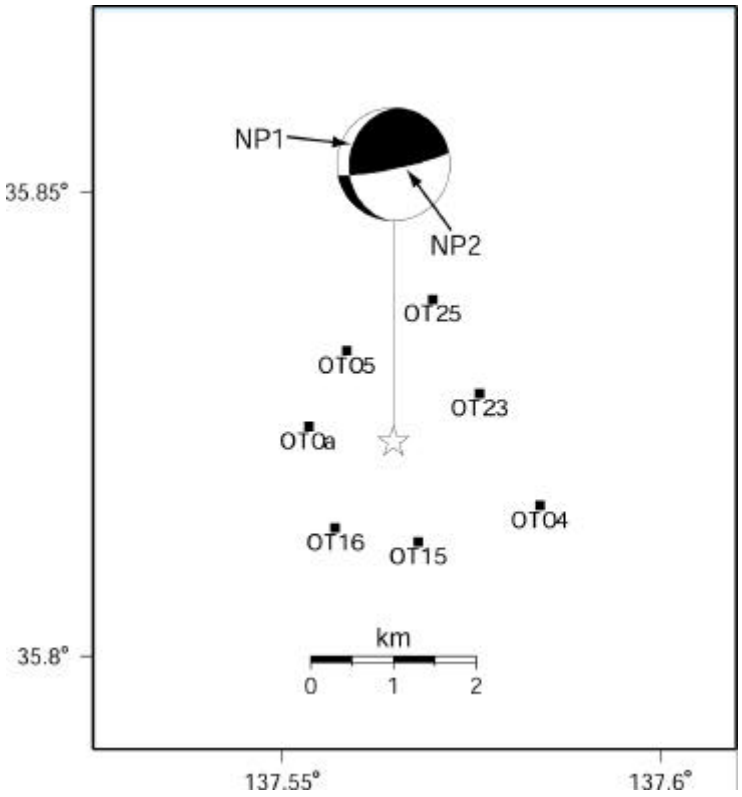

Location of the epicenter for the 1451 UT event of June 18, 1999 (star) and station distribution (squares). NP1 and NP2 signify two nodal planes, respectively.OTOa is GSJ 800 m deep borehole.

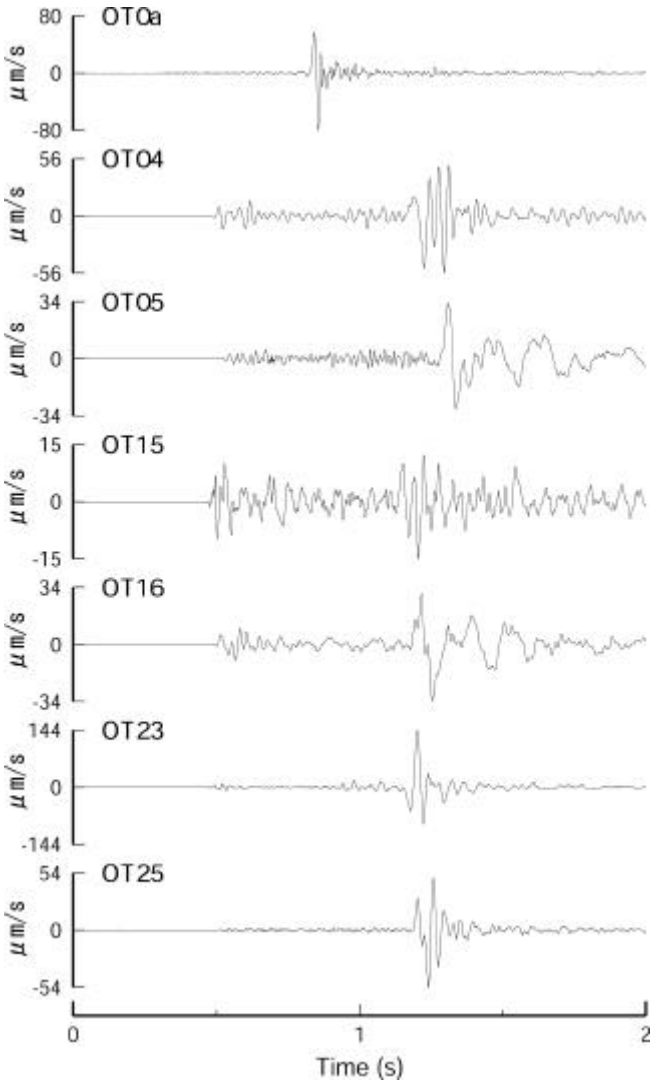

Velocity seismograms of SH component for the 1451 UT event of June 18, 1999.

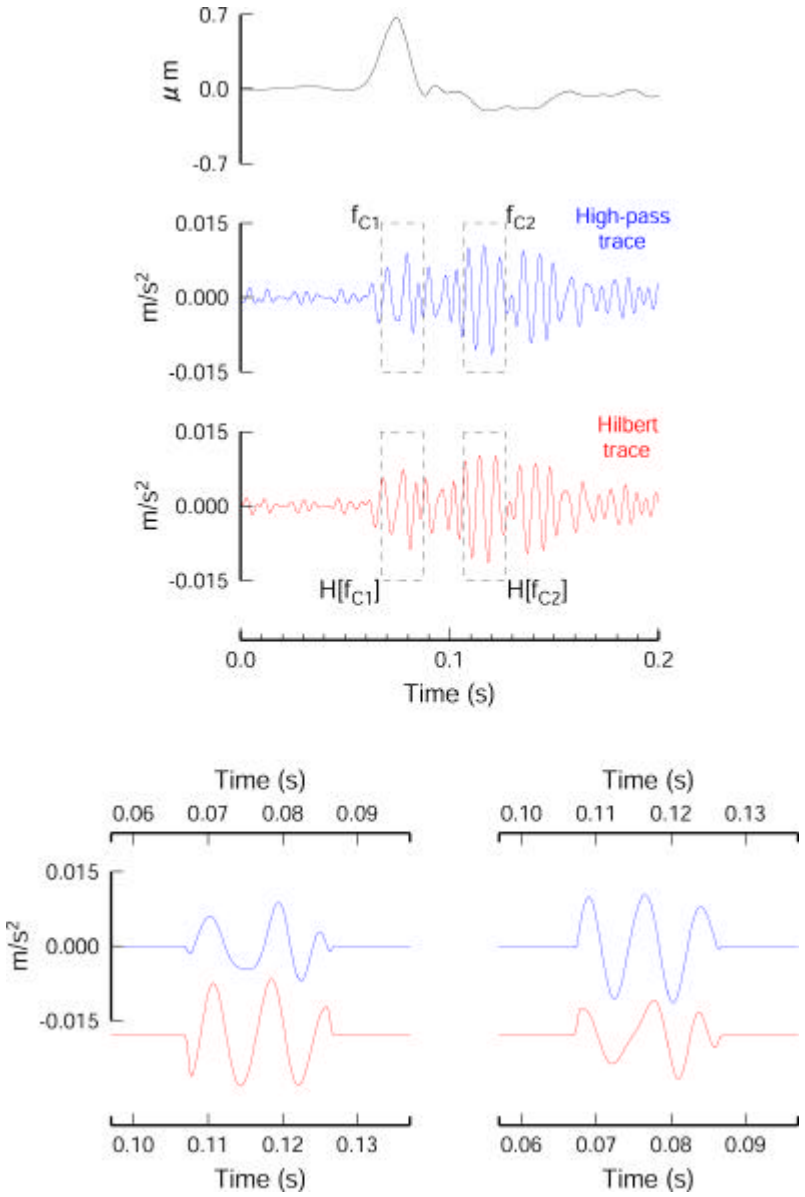

Comparison of the Hilbert transforms pairs of stopping phases for the 1451 UT event of June 18, 1999. The SH wave displacement is also shown. The waveforms in the C1 and C2 windows are enlarged in the lower half.

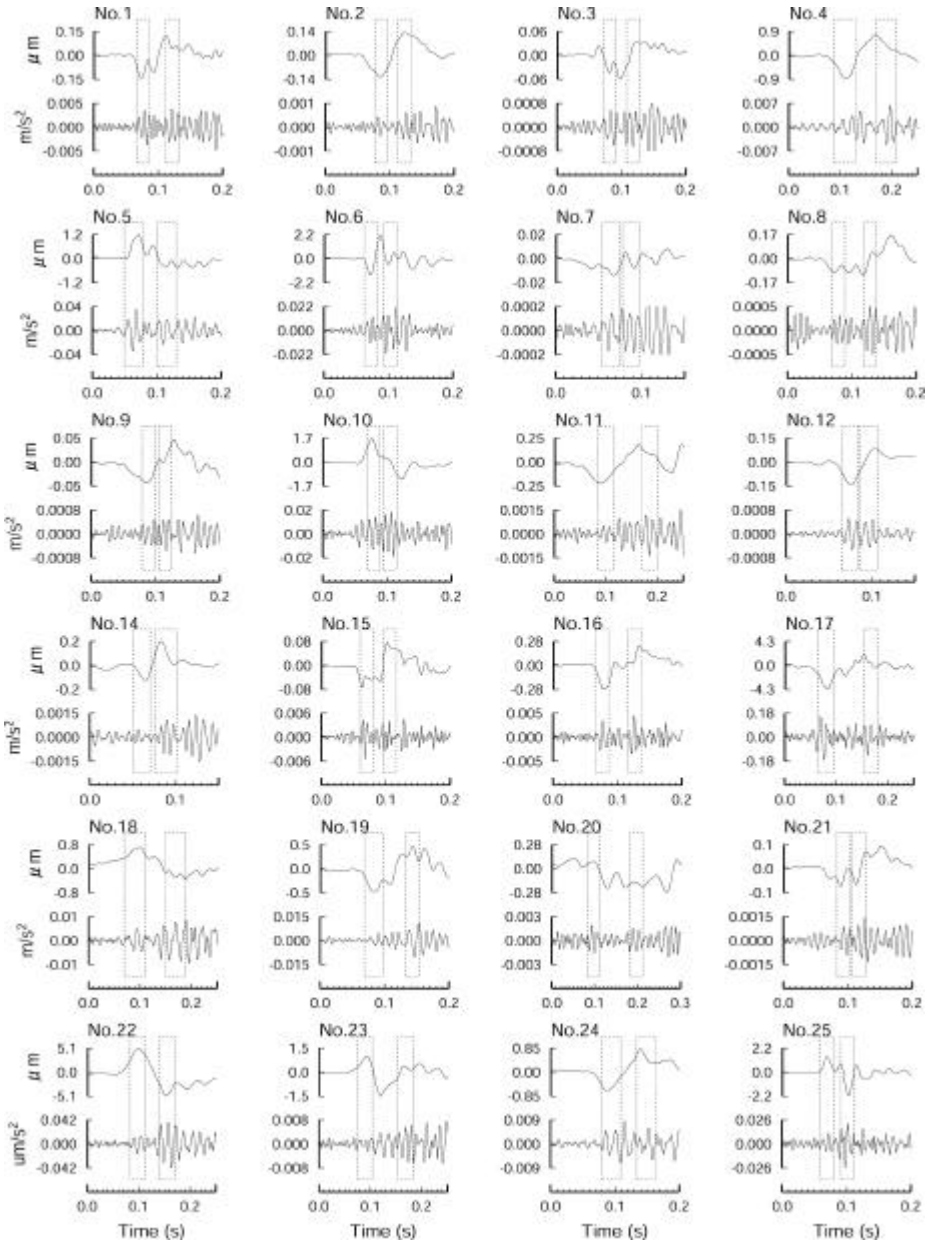

Comparisons of SH displacement seismograms with accelerograms. The dashed rectangles represent the timing of the two stopping phases.

Seismic moment versus rupture aspect ratio

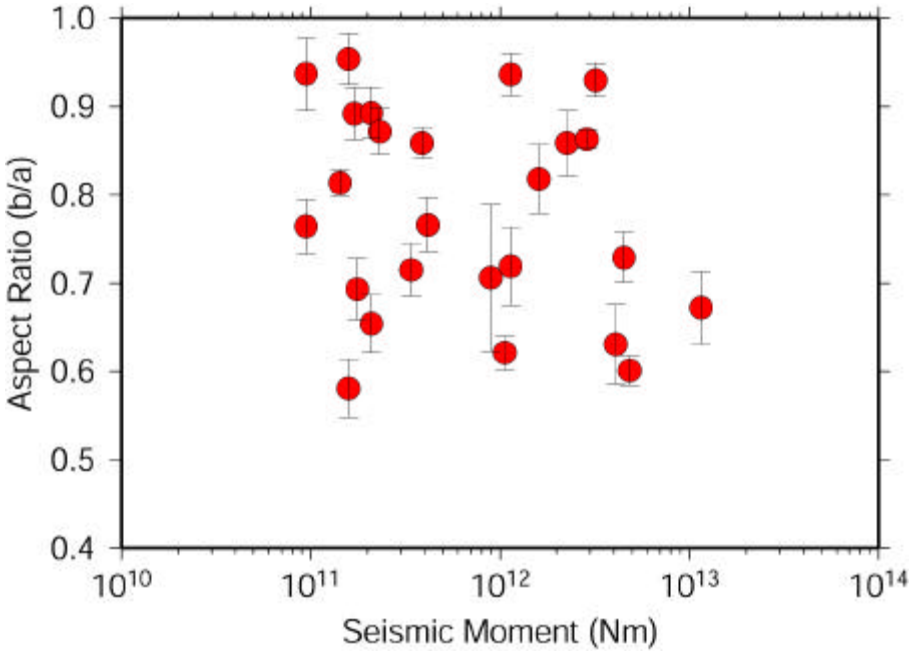

Seismic moment versus source dimension

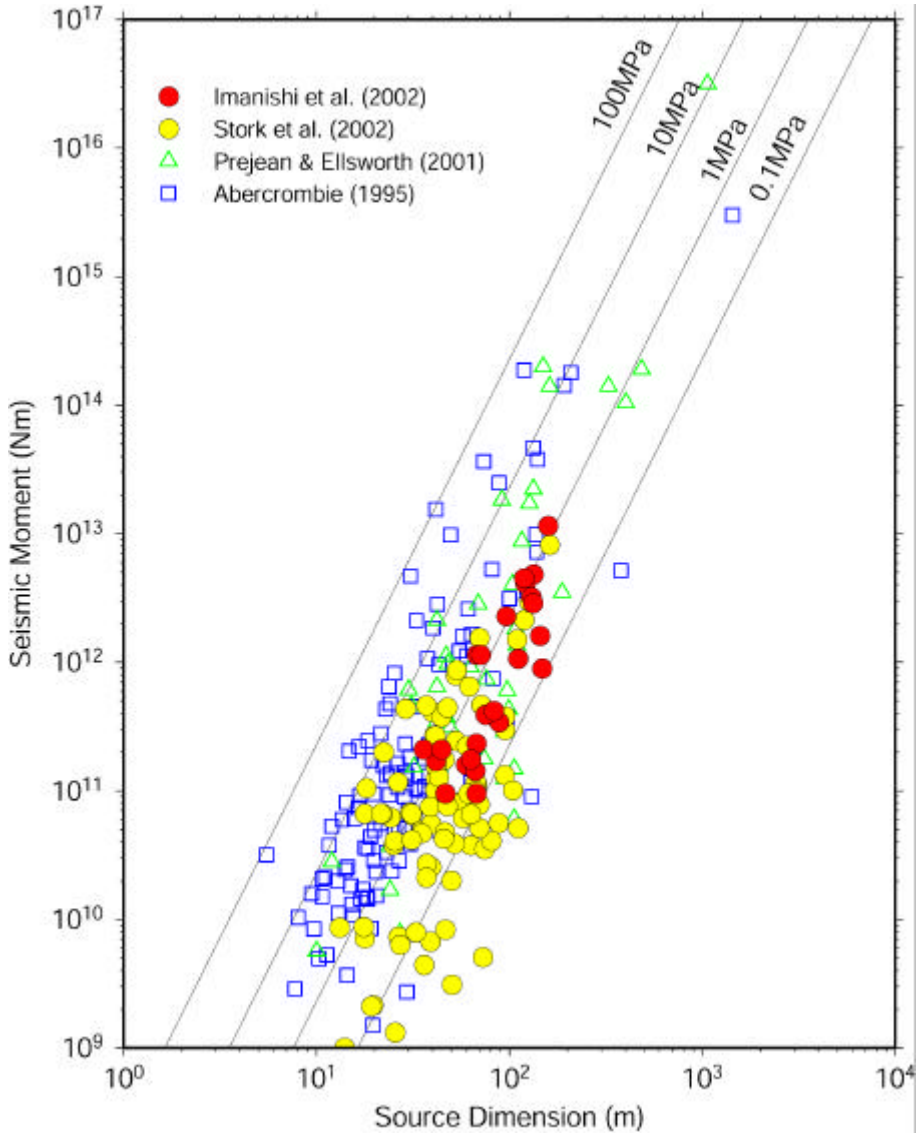

Seismic moment versus rupture velocity

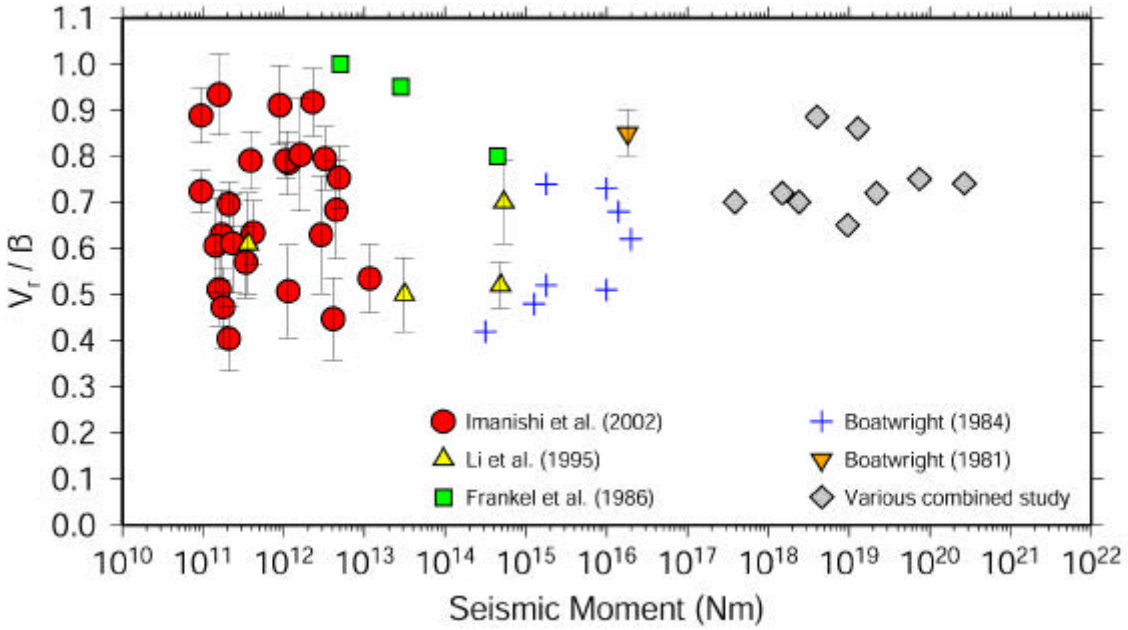

Seismic moment versus apparent stress

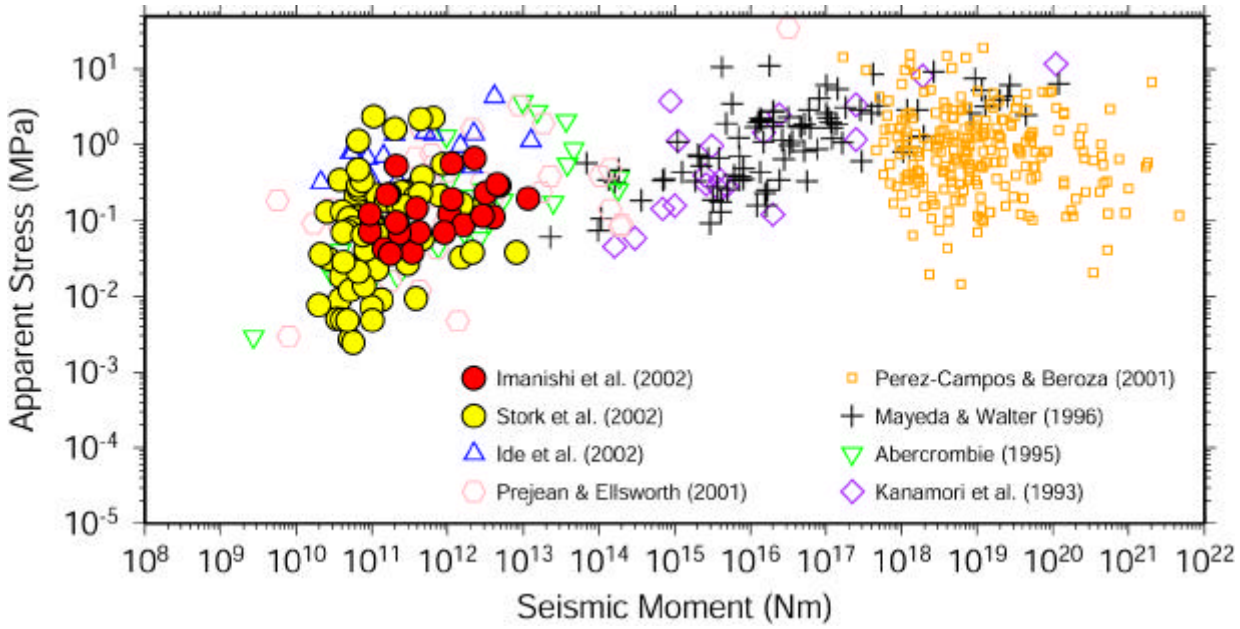

Conclusions (1)

- An inversion method using stopping phases has been applied to 25 small earthquakes ranging in size from M_w1.2 to 2.6 occurred at western Nagano prefecture, Japan.
- The 800 m borehole data provide a wide frequency bandwidth and greatly reduce ground noise and coda wave amplitude compared to surface recordings. High-frequency stopping phases, Hilbert transformations of each other, were readily detected on accelerograms recorded in the 800m borehole. As is expected from the synthetic waveforms, the first and secondary stopping phases arrive at around the maximum amplitude and the end of displacement pulse, respectively. This suggests that it is very effective in applying the present technique to small earthquakes.
- The rupture aspect ratio was estimated to be about 0.8 on an average, suggesting that the assumption of circular crack model is valid as a first order approximation for small earthquakes analyzed in this study.
- Static stress drops range from approximately 0.1 to 2 MPa and do not vary with seismic moment, source location and depth. The estimated values are slightly low compared to other tectonic earthquakes. Since the area is characterized by the persistent swarm activity, the low stress drop might suggest the weak strength of the rock materials in the area.
- The average values of rupture velocity do not depend on earthquake sizes, and are similar to those reported for moderate and large earthquakes. We then calculated the seismic energy following Sato and Hirasawa (1973). The magnitude scaling of the apparent stress is almost constant in the analyzed events, ranging from about 0.04 to 0.7 MPa. Since most of apparent stresses for large earthquakes are in the range of 0.1 to 10 MPa, there may be small differences in apparent stress between large and small earthquakes. However, it is likely that earthquakes are self-similar over a wide range of earthquake size and the dynamics of small and large earthquakes are similar from a macroscopic viewpoint.

Conclusions (2)

Both the spectrum analysis and stopping phase analysis show that it is likely that earthquakes are self-similar over a wide range of earthquake size and the dynamics of small and large earthquakes are similar from a macroscopic point of view.

Further studies

Technical problems

Recording limitations

P: 300 Hz, S: 200Hz

Directivity Effects?

Data

SAFOD

Constant Q

$$\Omega(f) = \frac{\Omega_0 \exp^{\frac{-pft}{Q}}}{\left[1+\left(f/f_c\right)^2\right]}$$

$$M_o = \frac{4prv^3 d\Omega_o}{F}$$ Brune (1970)

$$E_s = \frac{4prvd^2\langle F\rangle^2 \int \dot{u}^2 df}{F^2}$$ Boatwright and Fletcher (1984)

$$r = \frac{Cv}{2pf_c}$$

$$\Delta s_s = \frac{7M_0}{16r^3}$$

$$s_a = \frac{mE_s}{M_o}$$

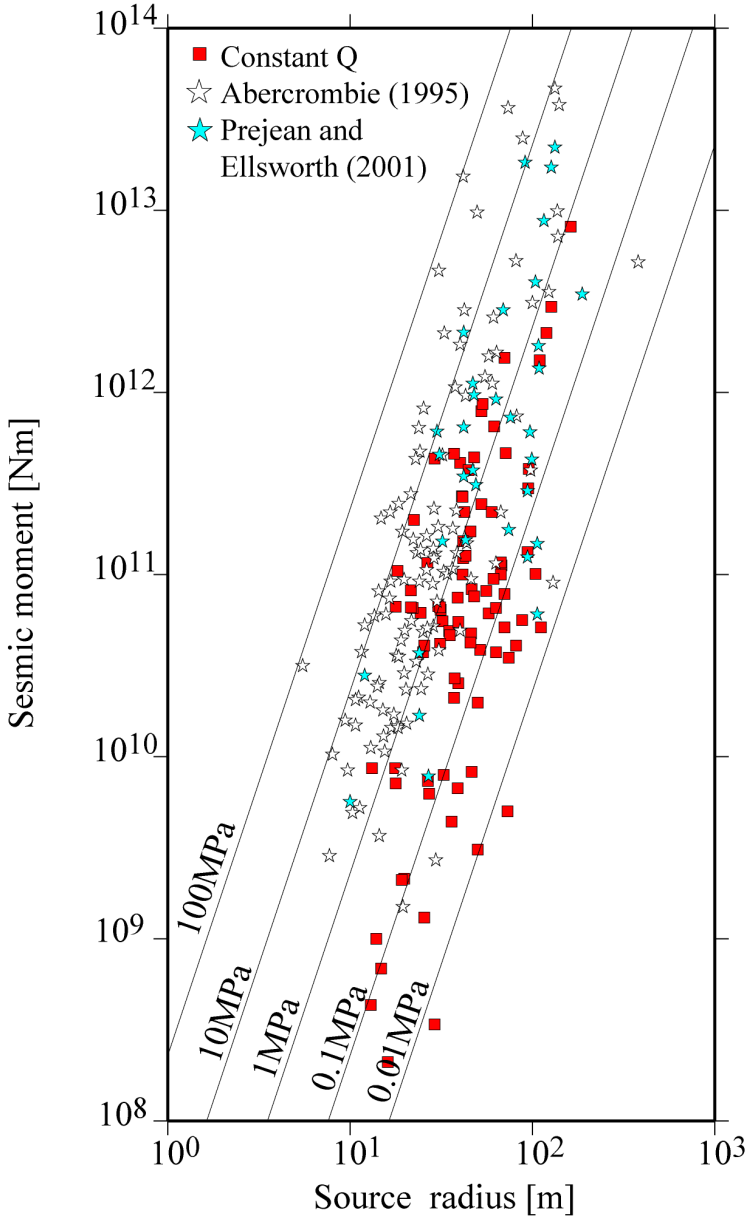
Constant Q
Abercrombie (1995)
Prejean and Ellsworth (2001)
100MPa
10MPa
1MPa
0.1MPa
0.01MPa
Sesmic moment [Nm]
Source radius [m]
10^14
10^13
10^12
10^11
10^10
10^9
10^8
10^0
10^1
10^2
10^3

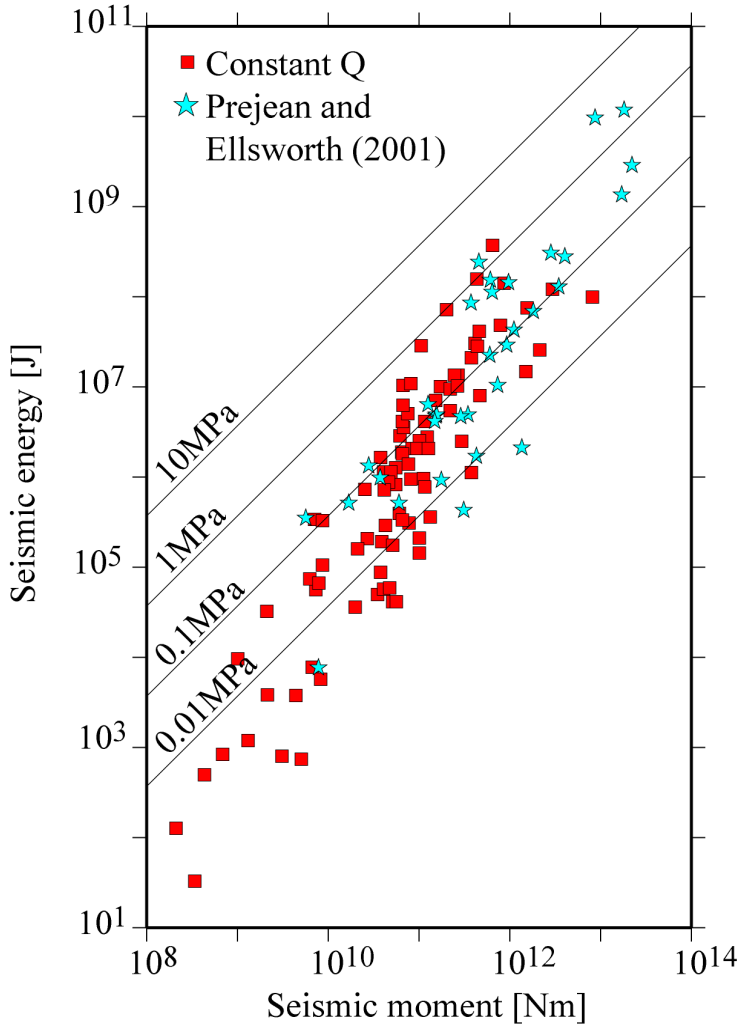
Constant Q
Prejean and Ellsworth (2001)
10MPa
1MPa
0.1MPa
0.01MPa
Seismic energy [J]
Seismic moment [Nm]
10^11
10^9
10^7
10^5
10^3
10^1
10^8
10^10
10^12
10^14

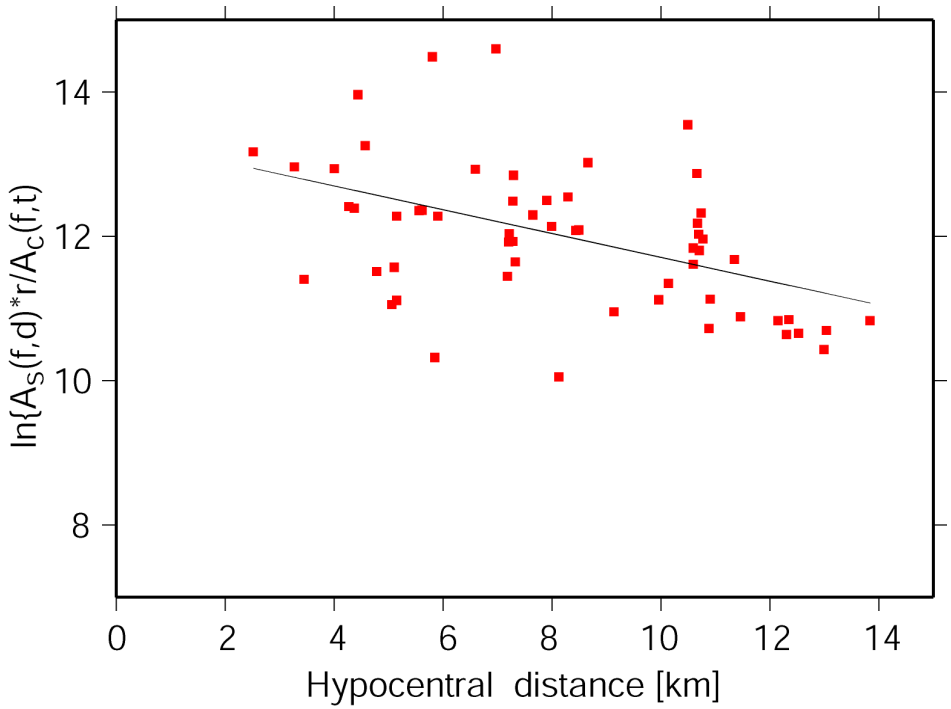
14
12
10
8
0
2
4
6
8
10
12
14
ln{A_S(f,d)*r/A_c(f,t)
Hypocentral distance [km]

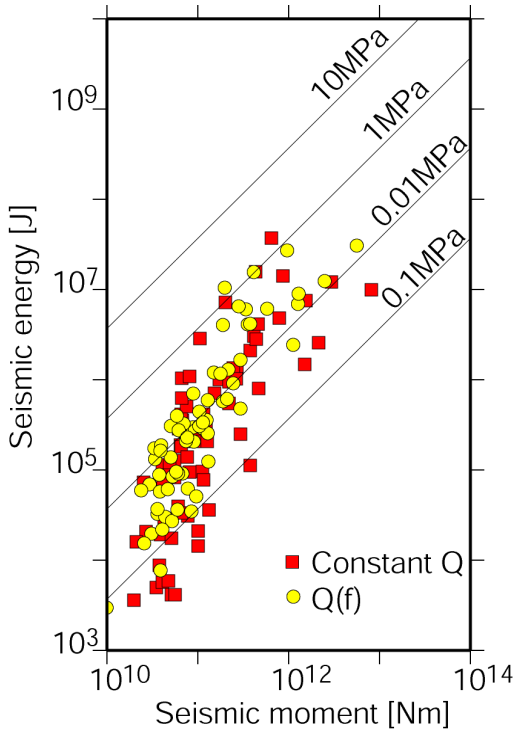
10MPa
1MPa
0.01MPa
0.1MPa
10^9
10^7
10^5
10^3
Seismic energy [J]
Constant Q
Q(f)
10^{10}
10^{12}
10^{14}
Seismic moment [Nm]

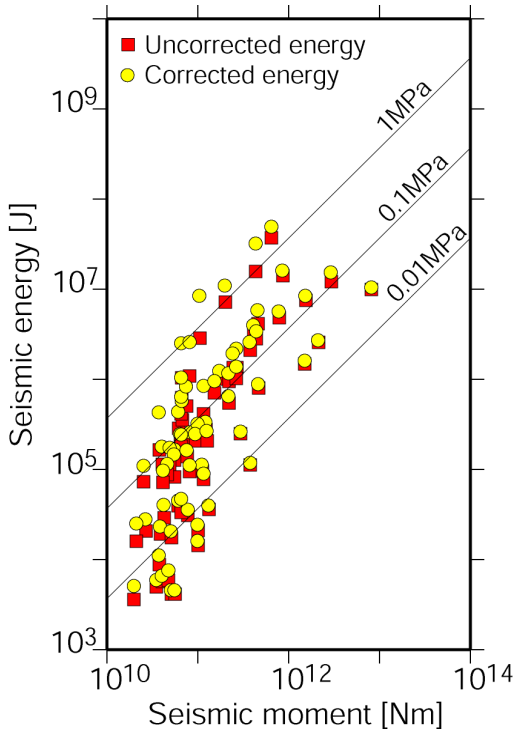
Uncorrected energy
Corrected energy
1MPa
0.1MPa
0.01MPa
10^9
10^7
10^5
10^3
Seismic energy [J]
10^{10}
10^{12}
10^{14}
Seismic moment [Nm]

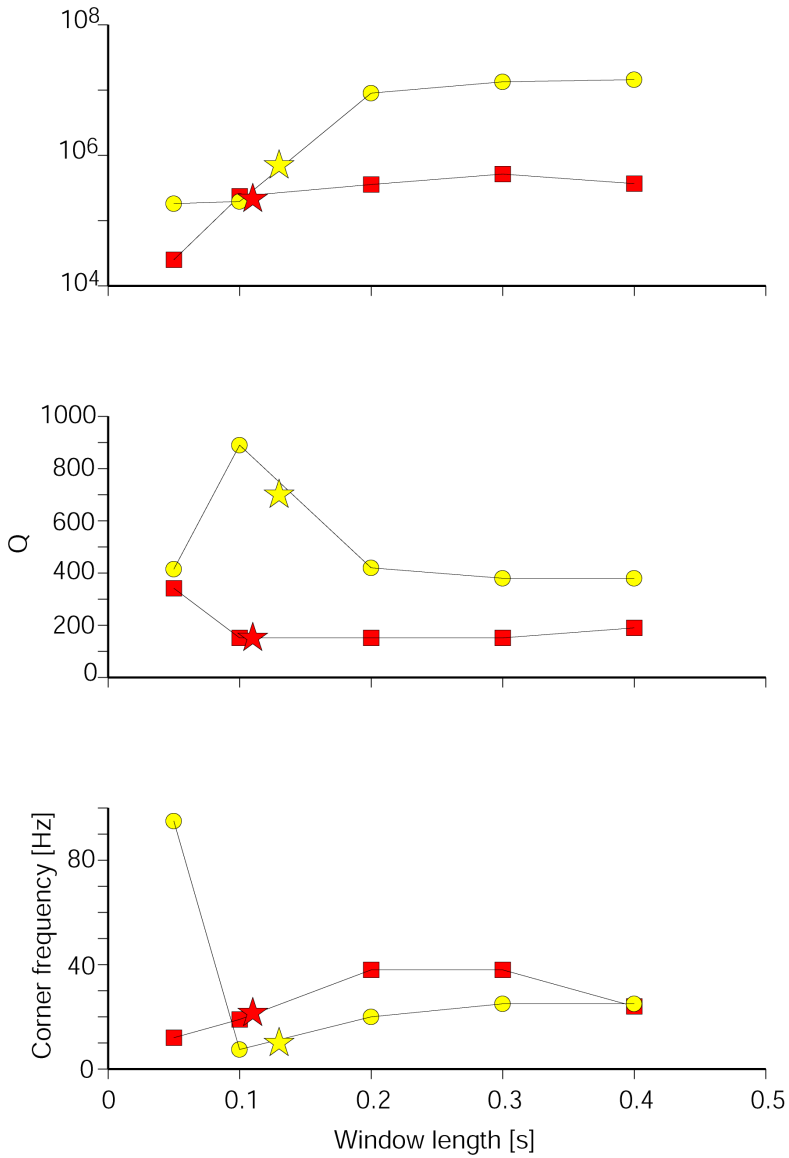
10^8
10^6
10^4
1000
800
600
400
200
0
Q
80
40
0
Corner frequency [Hz]
0
0.1
0.2
0.3
0.4
0.5
Window length [s]